

Article

Theoretical Analysis of a Molecular Optical Modulator for a Continuous-Wave Laser Based on a Hollow-Core Photonic Crystal Fiber

Shin-ichi Zaitzu^{1,2,*}, Takumi Tanabe¹, Kota Oshima¹ and Hiroyuki Hirata¹

¹ Department of Applied Chemistry, Graduate School of Engineering, Kyushu University, 744 Motooka, Nishi-ku, Fukuoka 819-0395, Japan; takumi.tanabe.387@s.kyushu-u.ac.jp (T.T.); k-oshima@cstf.kyushu-u.ac.jp (K.O.); h-hirata@cstf.kyushu-u.ac.jp (H.H.)

² Division of International Strategy, Center for Future Chemistry, Kyushu University, 744 Motooka, Nishi-ku, Fukuoka 819-0395, Japan

* Correspondence: s-zaitzu@cstf.kyushu-u.ac.jp; Tel.: +81-92-802-2884

Received: 22 August 2018; Accepted: 10 October 2018; Published: 12 October 2018



Abstract: A THz optical modulator for a continuous-wave laser using a hollow-core photonic crystal fiber (HC-PCF) was proposed and theoretically analyzed. Lightwaves traveling through the HC-PCF is modulated by interactions with coherently driven Raman-active molecules in the core. The coherent molecular motion is excited by a pulse train having an interval between successive pulses shorter than the molecular dephasing time. In principle, a rotational transition of molecular hydrogen ($S_0(1)$) at a pressure of 1 atm has a long enough dephasing time to maintain molecular coherence during a 1 GHz commercially available mode-locked pulse train. Optimization of the waveguide dispersion would enable phase-matching between the probe beam and generated sidebands during optical modulation. The proposed scheme would be achievable with a reasonable pump beam power and HC-PCF length, and with a feasible pressure of molecules in the core.

Keywords: optical modulation; hollow-core photonics crystal fiber; Raman scattering

1. Introduction

Advances in technologies to manipulate light have been reported for innovative uses in science and technology. Periodic or quasi-periodic light modulation plays important roles in spectroscopy, microscopy, optical information and communication technology, and ultrafast laser engineering [1,2]. Optical modulation is commonly achieved with acoustic- or electro-optical effects in solid-state crystals [3]. Frequencies have been limited to those of acoustic or high-voltage drivers, which are typically $\sim 10^7$ Hz or $\sim 10^{10}$ Hz at most, respectively. Methods to expand the frequency range include ultrafast Kerr effects in a silicon-polymer hybrid medium [4], recollisions of excitons in a quantum well structure [5], and a plasma wakefield of intense lasers [6]. These approaches, however, cannot operate at optical frequencies ($>10^{13}$ Hz), and new methods are required for future applications such as high-speed broadband optical communication systems.

Molecular optical modulation (MOM) is a promising way to realize operation at frequencies greater than 10 THz [7]. Molecules in a state of coherent motion can produce an ultrafast temporal variation of a refractive index in a macroscopic view [8]. The reflective index of the coherently excited molecular assembly oscillates at the same frequencies as the molecular motion and thus could modulate a light wave at the 10^{12} – 10^{14} Hz range. MOM has been demonstrated in the pulsed regime. Intense optical pulses have been used to coherently excite molecules, which modulated relatively weak optical pulses before the coherence totally decayed. MOM of continuous-wave (cw) light would have many applications, particularly for optical communication. However, there are

intrinsic difficulties in preparing the molecular coherence because of the relatively low intensities of cw lasers. A cw-MOM has been reported that used an optical cavity to enhance the intensities of the excitation beams [9], achieving MOM for a near-infrared cw laser with a efficiency greater than 10^{-4} [10]. In these approaches, however, bulky optical cavities were used that might limit future applications that require robust, compact devices.

A hollow-core photonics crystal fiber (HC-PCF) is a flexible component that is highly compatible with fiber-based optical systems that could improve information transduction capacity in current optical communication systems [11]. Gaseous media inside a fiber-core waveguide having a diameter of several to tens of μm can interact with relatively low intensity light propagating through the core, and produce nonlinear optical phenomena such as Raman scattering [12], four-wave mixing [13], and two-photon absorption [14]. The use of HC-PCFs for MOM has been reported in theoretical studies [15,16] and in experimental work [17,18], including few-cycle pulse generation [15] and supercontinuum up-conversion [17]. These reports used optical pulses for probing the molecular coherence, rather than low-intensity cw beams.

Here, a proposal is presented that takes advantage of HC-PCF as a waveguide for MOM of a cw laser based on Raman-active molecules in the core. A key idea is the use of a GHz pump beam train of ultrashort pulses to induce coherent motion of the molecules. The short interval time between successive pulses relative to the dephasing time of the molecular coherence would enable continuous excitation of the coherent motion. A theoretical analysis of the dependence of the molecular coherence amplitude on the pressure, the HC-PCF length, and the pump beam fluence indicates feasibility for 10-terahertz sideband generation for a cw probe beam under phase-matched conditions. This proposal can potentially lead to a fiber-based ultrafast optical modulator compatible with existing optical communication systems, and with the capacity to improve information transmission.

2. Theoretical Background

As shown in Figure 1, theoretical analysis of the proposed fiber-based MOM assumes an apparatus based on commercially available lasers to pump and probe gaseous Raman-active molecules in the HC-PCF. The HC-PCF is a photonic-bandgap type with a $<10\ \mu\text{m}$ diameter core, low-loss transmission at 800 nm and a $\sim 100\text{-nm}$ bandwidth. The pump beam is a 1-GHz mode-locked laser with an average power of a few watts (average energy of a few nJ) to excite coherent molecular motion in the HC-PCF. A 852-nm cw beam from a standard external-cavity laser diode is used to probe the molecular Raman coherence, leading to sideband generation in the MOM process.

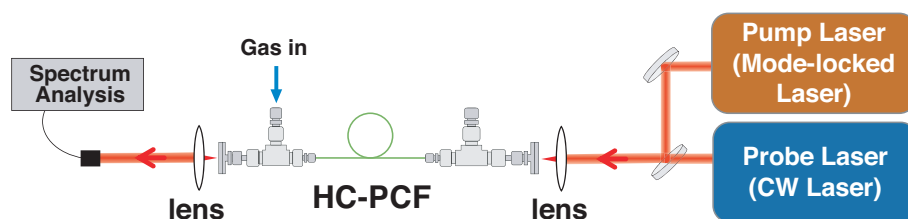


Figure 1. Experimental apparatus assumed in the theoretical analysis.

The amplitude of coherent molecular motion excited by the ultrashort pulses with a duration less than one period of the molecular motion can be expressed as:

$$Q(t) = Q_0 \exp\left(-\frac{t}{T_2}\right) \sin(\Omega t), \quad (1)$$

where T_2 is the dephasing time of the molecular coherence and Ω is the frequency of molecular motion. The initial amplitude, Q_0 when molecules are excited by the pump pulse at $t = 0$ was determined by the fluence of the pump pulse energy F_p :

$$Q_0 = \frac{2\pi}{Mc\Omega} \left\{ \frac{\partial\alpha}{\partial Q} \right\} F_p, \quad (2)$$

where M is the effective molecular mass and $\partial\alpha/\partial Q$ is the change in polarizability with respect to the molecular coordinates. In Equation (2), larger coherent molecular motion is obtained when the pump pulse fluence is larger, i.e., larger energy per a unit area [19].

When a probe beam given by $\varepsilon_i(z, t) = (1/2)E_i \exp i(\omega_i t - k_i z) + c.c.$ propagates through the coherently excited molecules, the molecular motion affects its electromagnetic field via the nonlinear polarizability $P_R = N(\partial\alpha/\partial Q)Q(t)E_i$, where N is the molecular density. From the solution of the wave equation including the nonlinear polarizability, the amplitude of the electromagnetic field of the probe beam E_i propagating through the coherently oscillating molecules at distance l is:

$$E_i(z, t) = E_i(0, t) \exp \{-i\beta l \sin(\Omega t)\}. \quad (3)$$

It is assumed that the phase-mismatch caused by the difference between the pump and probe phase velocities is negligibly small. Equation (3) is valid when dephasing of the molecular coherence during the period between successive pump pulses is negligible (see Discussion). β is a parameter corresponding to the Raman gain in stimulated Raman scattering given by:

$$\beta = \frac{2\pi\omega_i N}{c} \left\{ \frac{\partial\alpha}{\partial Q} \right\} Q_0 \quad (4)$$

Equation (4) is consistent with increased Raman gain with the amplitude of molecular coherence.

The spectrum of the probe beam after interaction with the molecules is obtained by the Fourier transform of Equation (4):

$$|F_i(\delta\omega)|^2 = \sum_{n=-\infty}^{\infty} |f_i(\delta\omega - n\Omega)|^2 \cdot J_n^2(\xi), \quad (5)$$

where $\xi = \beta l$, and $J_n(\xi)$ is an n -th order Bessel function. Here, $f_i(\delta\omega) = f_i(\omega - \omega_i)$ is an initial spectrum that is an extremely narrow line at $\delta\omega = 0$ for a cw laser beam. Equation (5) reveals a comb-like spectrum with equally-spaced lines separated by Ω that is symmetrical about the initial probe frequency. The intensities of the 0-th order component and the n -th order sidebands are determined by the n -th order Bessel function, $J_n(\xi)$, $n = \pm 0, 1, 2, \dots$. The parameter ξ is derived from Equations (2) and (4):

$$\xi = \frac{4\pi^2\omega_i}{Mc^2\Omega} \left(\frac{\partial\alpha}{\partial Q} \right)^2 \cdot N \cdot F_p \cdot l. \quad (6)$$

Equation (6) indicates that the sideband intensities arising from the MOM depended on three controllable factors: (1) the density of molecules N , (2) the fluence of the pump beam F_p , and (3) the length of the interaction l . This also suggests that the optical modulation based on coherent motion of molecules in the HC-PCF benefits from a long fiber length (>10 m) for light-molecule interactions. In addition, tight focusing of the pump beam into the core (several μm) enables an increased energy density for coherent molecular excitation.

3. Results

The evolution of the sidebands was estimated by the increase of ξ within a reasonably available range. Figure 2a plots the depletion of the fundamental component and the growth of the sidebands ($n = \pm 1, \pm 2, \pm 3$) as a function of ξ calculated by Equation (6). Thus, the power of the 0-th order fundamental component was converted into higher order sidebands sequentially with increasing ξ . Figure 2b plots the spectrum of a probe beam optically modulated by coherently excited molecules for $\xi = 1$. The intensity of the 0-th order component was 0.586, whereas those of the ± 1 -st and ± 2 -nd-order sidebands were 0.194 and 0.013, respectively. The intensities of the ± 2 -nd-order sidebands for $\xi = 1$

were sufficient to provide a high signal-to-noise ratio for some applications, e.g., phase-locking of a multifrequency laser [20]. Figure 2b also plots the sideband intensities with the same absolute values for each order, e.g., $n = +1$ and -1 , were equal. Actually, the dispersions of the waveguide and the gaseous medium produced a slight asymmetry between the Stokes and anti-Stokes sidebands because the anti-Stokes sideband generation depended on the phase mismatch between the fundamental and the sidebands. In this calculation, perfect phase-matching was assumed for the sideband generation. Hence, this result was valid only when the fundamental frequency had zero-dispersion in the HC-PCF [21].

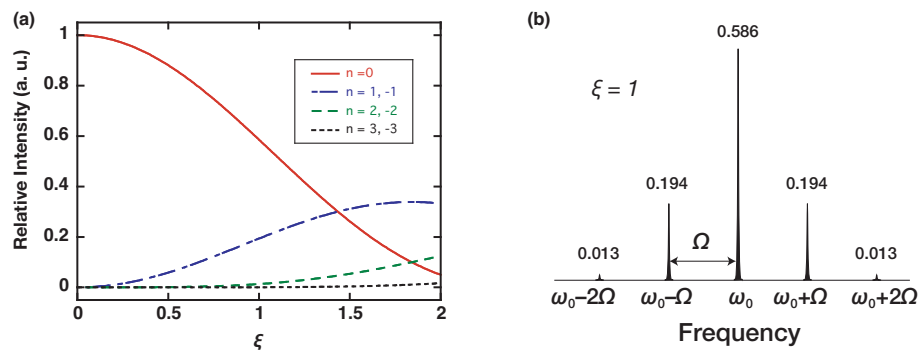


Figure 2. (a) Dependence of intensities of the pump beam ($n = 0$) and the n -th-order sidebands ($n = \pm 1, \pm 2, \pm 3$) on ξ . (b) Spectrum for $\xi = 1$ when the pump beam frequency was ω_0 and the modulation frequency was Ω .

The parameter ξ was estimated using Equation (6) for reasonable ranges of those parameters to achieve MOM with molecular hydrogen. The modulation was based on the rotational transition of *ortho*-hydrogen ($S_0(1), J = 1 \rightarrow J = 3$), that produced a modulation frequency, Ω , of 17.6 THz. This was used previously [9,10] for MOM of a cw laser in a high-finesse optical cavity filled with hydrogen. The 852-nm probe beam was a commercially available laser diode. The pump beam was an ultrashort 30-fs optical pulse that was less than one 57-fs rotational period of the hydrogen molecule, and had a ~ 25 -nm full-width at half-maximum spectral bandwidth. Thus, it created coherent molecular motion efficiently [22]. The 852-nm center wavelength of the pump beam was the same wavelength as that of the probe beam. However, the transverse modes of both the pump and probe beams had the lowest mode of a Gaussian shape, with beam diameters of 10 μm at $1/e^2$ intensity, which was similar to the core diameters of typical HC-PCFs. The specific parameter of a hydrogen molecule that determines its Raman polarizability, $\partial\alpha/\partial Q$, was assumed to be 2.6×10^{-17} , which was estimated from an experimental rotational Raman gain coefficient [23].

Figure 3a shows the dependence of ξ on the power of the pump pulse P (W) in the core of a 10-m-long HC-PCF for hydrogen pressures ρ of 1, 5, and 10 atm. The figure shows that the input pump power that equaled ξ decreased inversely proportional to the pressure. However, lower pressures were more desirable to suppress relaxation of the excited molecular coherence, as discussed below. ξ reached 1 for a 4.5-W input pump power when the pressure was 1 atm. Increasing the length of the HC-PCF contributed to the reduction of the pump power and the hydrogen pressure; Figure 3b plots the dependence of the product $P \times \rho$ (W·atm) on the length of the HC-PCF, l (m). For $l = 50$, $\xi = 1$ was attained by $P \times \rho = 0.91$, which meant that input pump beam less than 1 W was sufficient to produce sidebands with intensities shown in Figure 2b at a hydrogen pressure of 1 atm. A longer HC-PCF would be a much more effective way to reduce the cost of the apparatus than increasing the pump beam power. However, a longer HC-PCF would make it more difficult to satisfy the MOM phase-matching conditions. This problem is addressed below in the Discussion section.

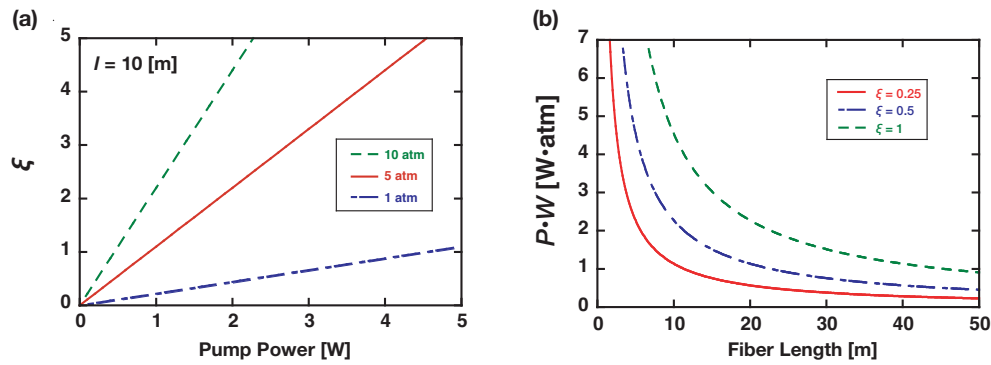


Figure 3. (a) Evolution of ζ as a function of pump beam power for hydrogen pressures of 1, 5, 10 atm in a 10-m HC-PCF. (b) Dependence on the HC-PCF length of the product of the pump power and the hydrogen pressure needed to satisfy $\zeta = 0.25, 0.5, 1$.

Figure 4 shows contour curves plotted at $\zeta = 0.25, 0.5, 1$ as a function of hydrogen pressure in the HC-PCF ρ (atm), the length of the HC-PCF l (m), and the input power of the pump beam P (W). The parameters ranged from 0 to 10 atm for ρ , from 0 to 10 m for l , and from 0 to 1 W for P . ρ was assumed to be proportional to the molecular density N (cm^{-3}). $\zeta = 1$ was sufficiently achievable for the parameter ranges in this calculation, e.g., a ~ 25 -m HC-PCF length enabled $\zeta = 1$ for $\rho = 1$ (atm) and $P = 2$ (W). The parameters ranges were experimentally feasible with commercially available equipment, indicating that the proposed idea was promising. In the MOM system based on a dispersion-compensated optical cavity reported elsewhere [10], ζ was estimated to be 0.17 at a pump power of 0.35 W. The results for the MOM based on a HC-PCF shown here implies that the HC-PCF system has a potential to overcome the optical-cavity-based system in the efficiency of the generation of the sidebands for a pump power less than 1 W.

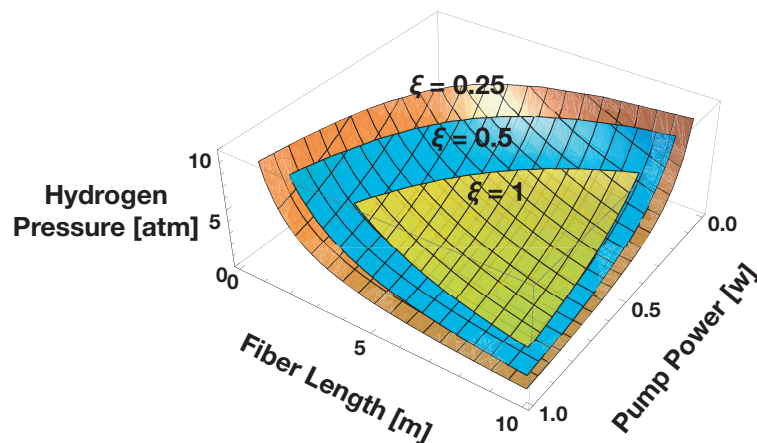


Figure 4. Contour curves for $\zeta = 0.25, 0.5, 1$ as a function of hydrogen pressure, the hollow-core photonic crystal fiber (HC-PCF) length, and the pump power.

4. Discussion

Two important issues are: (1) relaxation of the molecular coherence, and (2) phase-mismatching between the probe beam and the MOM-generated sidebands, as well as that between the probe and pump beams. The coherent motion of molecules is excited by a train of ultrashort pulses, and is probed with a cw laser. The coherence decays with a certain time constant until the next incoming pulse restored it. Hence, the time interval between pulses is a critical factor that determined the amplitude of the coherent molecular motion. By using a 1 GHz mode-locked pump source, the dephasing time of

the molecular coherence is assumed to be longer than 1 ns. The dephasing time T_2 of the molecular coherence is given by:

$$T_2 = \frac{1}{\pi\Gamma}, \quad (7)$$

where Γ is the Lorentzian linewidth of the Raman gain curve. This relationship is satisfied for rotational Raman scattering of hydrogen in a pressure range of 0.5 atm to several atm, and Γ has a linear dependence on pressure (or concentration). Previously [24], Γ was expressed as: $\Gamma(\rho) = 97.3\rho$ (MHz), where ρ was the hydrogen pressure (atm). This immediately results in $T_2 = 3.2/\rho$ (ns), which indicates that the hydrogen pressure should be ideally ~ 1 atm to maintain molecular coherence until the next pump pulse. There is a trade-off between repetition rate and pump energy, although increased energy contributes to increased excitation of coherent molecular motion.

The phase-matching condition $\Delta k = 0$ leads to maximum optical modulation. Larger Δk dramatically reduces the MOM efficiency and directly suppresses the sidebands intensities. The MOM Δk is approximately $\Delta k = Df$, where D is a group delay dispersion of the modulation medium and f is the modulation frequency [25]. Although Δk can be negligible for f in the GHz range, an extremely high modulation frequency (larger than 10 THz) causes significant effects [10]. To satisfy $\Delta k = 0$, the elimination of the medium dispersion, i.e., $D = 0$, is required. This is difficult because gaseous media at a few atm usually produce dispersions at optical frequencies that are non-negligible for optical modulation greater than 10 THz. In addition, the medium dispersion is proportional to HC-PCF length. Thus, a longer HC-PCF leads to a larger dispersion, i.e., a larger Δk in the MOM process. This problem could be solved by the control of the total dispersion of the medium-filled HC-PCF that is determined by the sum of the contributions from the medium and the waveguide. Typical HC-PCFs have a transmission band with a negative waveguide dispersion [26]. Thus, the sign of HC-PCF dispersion is opposite to that of the medium filling the HC-PCF. The positive dispersion of the medium can be offset by the negative dispersion of the HC-PCF. This would allow the total dispersion to be virtually zero at a frequency of the probe beam for MOM, by using an optimized medium pressure. Kagome-type HC-PCFs may benefit from less frequency-dependent dispersion compared with photonic-bandgap HC-PCFs [27]. Under those conditions, phase matching of the optical modulation would be satisfied, leading to efficient modulation of the probe beam at a frequency greater than 10 THz.

5. Conclusions

An optical modulator for a cw beam has been theoretically proposed that operated at more than 10 THz. It used a HC-PCF waveguide to contain gaseous Raman-active molecules. A GHz mode-locked laser was assumed to excite coherent motion of hydrogen molecules in the HC-PCF core, and a single-frequency semiconductor laser probed the coherently driven molecular oscillation. In this scheme, the probe beam could be modulated at a terahertz frequency corresponding to rotation hydrogen motion. The amplitude was calculated for the coherence of the $S_0(1)$ transition of molecular hydrogen excited by an ultrashort optical pulse having a duration less than one period of molecular motion. Feasible conditions were presented that could produce sufficient coherence to enable the MOM, i.e., the generation of sidebands, for a cw probe beam. The dephasing time of the molecular coherence was almost negligible at a certain pressure and a 1-GHz-repetition-rate pump rate. Phase-matching in the MOM process could be achieved by adequate control of the HC-PCF waveguide dispersion that compensated for dispersion by the gaseous molecules. The proposed scheme would be a milestone in the development of ultrafast optical modulators for high-capacity communication systems.

Author Contributions: Conceptualization, S.Z.; data curation, S.Z.; formal analysis, S.Z.; funding acquisition, S.Z.; investigation, S.Z., T.T., K.O. and H.H.; writing original draft, S.Z.; review and editing, S.Z.

Funding: This research was partly supported by a Grant-in-Aid for Scientific Research from the Japan Society for the Promotion of Science (JSPS KAKENHI, Grant No. JP18K04982) (S. Zaitzu), research grants from The Mazda Foundation (S. Zaitzu) and The Murata Science Foundation (S. Zaitzu).

Acknowledgments: We thank Alan Burns, from the Edanz Group (www.edanzediting.com/ac) for editing a draft of this manuscript.

Conflicts of Interest: The authors declare no conflict of interest.

References

1. Sun, Z.; Martinez, A.; Wang, F. Optical Modulators with 2D Layered Materials. *Nat. Photonics* **2016**, *10*, 227–238. [[CrossRef](#)]
2. Reed, G.T.; Mashanovich, G.; Gardes, F.Y.; Thomson, D.J. Silicon Optical Modulators. *Nat. Photonics* **2010**, *4*, 518–526. [[CrossRef](#)]
3. Liu, K.; Ye, C.R.; Khan, S.; Sorger, V.J. Review and Perspective on Ultrafast Wavelength-Size Electro-Optic Modulators. *Laser Photonics Rev.* **2015**, *9*, 172–194. [[CrossRef](#)]
4. Hochberg, M.; Baehr-Jones, T.; Wang, G.; Shearn, M.; Harvard, K.; Luo, J.; Chen, B.; Shi, Z.; Lawson, R.; Sullivan, P.; et al. Terahertz All-Optical Modulation In a Silicon-Polymer Hybrid System. *Nat. Mater.* **2006**, *5*, 703–709. [[CrossRef](#)] [[PubMed](#)]
5. Zaks, B.; Liu, R.B.; Sherwin, M.S. Experimental Observation of Electron-Hole Recollisions. *Nature* **2012**, *483*, 580–583. [[CrossRef](#)] [[PubMed](#)]
6. Yu, L.L.; Zhao, Y.; Qian, L.J.; Chen, M.; Weng, S.M.; Sheng, Z.M.; Jaroszynski, D.A.; Mori, W.B.; Zhang, J. Plasma Optical Modulators for Intense Lasers. *Nat. Commun.* **2016**, *7*, 11893. [[CrossRef](#)] [[PubMed](#)]
7. Baker, S.; Walmsley, I.A.; Tisch, J.W.G.; Marangos, J.P. Femtosecond to Attosecond Light Pulses from a Molecular Modulator. *Nat. Photonics* **2011**, *5*, 664–671. [[CrossRef](#)]
8. Garmire, E.; Pandarese, F.; Townes, C.H. Coherently Driven Molecular Vibrations and Light Modulation. *Phys. Rev. Lett.* **1963**, *11*, 160–163. [[CrossRef](#)]
9. Weber, J.J.; Green, J.T.; Yavuz, D.D. 17 THz Continuous-Wave Optical Modulator. *Phys. Rev. A* **2012**, *85*, 013805. [[CrossRef](#)]
10. Zaitsu, S.; Izaki, H.; Tsuchiya, T.; Imasaka, T. Continuous-Wave Phase-Matched Molecular Optical Modulator. *Sci. Rep.* **2016**, *6*, 20908. [[CrossRef](#)] [[PubMed](#)]
11. Gao, S.F.; Wang, Y.Y.; Ding, W.; Jiang, D.L.; Gu, S.; Zhang, X.; Wang, P. Hollow-core conjoined-tube negative-curvature fibre with ultralow loss. *Nat. Commun.* **2018**, *9*, 2828. [[CrossRef](#)] [[PubMed](#)]
12. Benabid, F.; Knight, J.C.; Antonopoulos, G.; Russell, P.S.J. Stimulated Raman Scattering in Hydrogen-Filled Hollow-Core Photonic Crystal Fiber. *Science* **2002**, *298*, 399–402. [[CrossRef](#)] [[PubMed](#)]
13. Londero, P.; Venkataraman, V.; Bhagwat, A.R.; Slepko, A.D.; Gaeta, A.L. Ultralow-Power Four-Wave Mixing with Rb in a Hollow-Core Photonic Band-Gap Fiber. *Phys. Rev. Lett.* **2009**, *103*, 043602. [[CrossRef](#)] [[PubMed](#)]
14. Venkataraman, V.; Saha, K.; Londero, P.; Gaeta, A.L. Few-Photon All-Optical Modulation in a Photonic Band-Gap Fiber. *Phys. Rev. Lett.* **2011**, *107*, 193902. [[CrossRef](#)] [[PubMed](#)]
15. Huang, Z.; Wang, D.; Londero, P.; Leng, Y.; Dai, Y. Few-Cycle Laser Pulses Generation with Frequency Tuning in a Molecular Gas-Filled Hollow-Core Fiber. *Opt. Express* **2015**, *23*, 17711–17719. [[CrossRef](#)] [[PubMed](#)]
16. Saleh, M.F.; Wang, D.; Armadori, A.; Marini, A.; Biancalana, F. Strong Raman-Induced Noninstantaneous Soliton Interactions in Gas-Filled Photonic Crystal Fibers. *Opt. Lett.* **2015**, *40*, 4058–4061. [[CrossRef](#)] [[PubMed](#)]
17. Bauerschmidt, S.T.; Novoa, D.; Trabold, B.M.; Abdolvand, A.; Russell, P.S.J. Supercontinuum Up-Conversion via Molecular Modulation in Gas-Filled Hollow-Core PCF. *Opt. Express* **2014**, *22*, 20566–20573. [[CrossRef](#)] [[PubMed](#)]
18. Husakou, A.; Wang, Y.Y.; Armadori, A.; Alharbi, M.; Benabid, F. Spatiotemporal Dynamics of Raman Coherence in Hollow-Core Fibers For a Pump-Probe Setup. *Phys. Rev. A* **2018**, *97*, 023814. [[CrossRef](#)]
19. Nazarkin, A.; Korn, G.; Wittmann, M.; Elsaesser, T. Generation of Multiple Phase-Locked Stokes and Anti-Stokes Components in an Impulsively Excited Raman Medium. *Phys. Rev. Lett.* **1999**, *83*, 2560–2563. [[CrossRef](#)]
20. Wu, D.S.; Richardson, D.J.; Slavík, R. Optical Fourier Synthesis of High-Repetition-Rate Pulses. *Optica* **2015**, *2*, 18–26. [[CrossRef](#)]
21. Benabid, F.; Roberts, P.J. Linear and Nonlinear Optical Properties of Hollow Core Photonic Crystal Fiber. *J. Mod. Opt.* **2011**, *58*, 87–124. [[CrossRef](#)]

22. Korn, G.; Dühr, O.; Nazarkin, A. Observation of Raman Self-Conversion of fs-Pulse Frequency due to Impulsive Excitation of Molecular Vibrations. *Phys. Rev. Lett.* **1998**, *81*, 1215–1218. [[CrossRef](#)]
23. Meng, L.S.; Roos, P.A.; Carlsten, J.L. Continuous-Wave Rotational Raman Laser in H₂. *Opt. Lett.* **2002**, *27*, 1226–1228. [[CrossRef](#)] [[PubMed](#)]
24. Herring, G.C.; Dyer, M.J.; Bischel, W.K. Temperature and Density Dependence of the Linewidths and Line Shifts of the Rotational Raman Lines in N₂ and H₂. *Phys. Rev. A* **1986**, *34*, 1944–1951. [[CrossRef](#)]
25. Agrawal, G. *Nonlinear Fiber Optics*; Academic Press: San Diego, CA, USA, 2012.
26. Bouwmans, G.; Luan, F.; Knight, J.C.; Russell, P.S.J.; Farr, L.; Mangan, B.J.; Sabert, H. Properties of a Hollow-Core Photonic Bandgap Fiber at 850 nm Wavelength. *Opt. Express* **2003**, *11*, 1613–1620. [[CrossRef](#)] [[PubMed](#)]
27. Im, S.J.; Husakou, A.; Herrmann, J. Guiding Properties and Dispersion Control of Kagome Lattice Hollow-Core Photonic Crystal Fibers. *Opt. Express* **2009**, *17*, 13050–13058. [[CrossRef](#)] [[PubMed](#)]



© 2018 by the authors. Licensee MDPI, Basel, Switzerland. This article is an open access article distributed under the terms and conditions of the Creative Commons Attribution (CC BY) license (<http://creativecommons.org/licenses/by/4.0/>).